Time-Hopping Multiple-Access for Backscatter Interference Networks

Wanchun Liu*, Kaibin Huang†, Xiangyun Zhou*, and Salman Durrani*,
*School of Electrical and Information Engineering, The University of Sydney, Sydney, Australia
†The Dept. of EEE, The University of Hong Kong, Hong Kong
*Research School of Engineering, The Australian National University, Canberra, Australia
Corresponding author email: wanchun.liu@sydney.edu.au

***Abstract*— Future *Internet-of-Things* (IoT) is expected to wirelessly connect tens of billions of low-complexity devices. Extending the finite battery life of massive number of IoT devices is a crucial challenge. The ultra-low-power *backscatter communications* (BackCom) with the inherent feature of RF energy harvesting is a promising technology for tackling this challenge. Moreover, many future IoT applications will require the deployment of dense IoT devices, which induces strong interference for wireless *information transfer* (IT). To tackle these challenges, in this paper, we propose the design of a novel multiple-access scheme based on *time-hopping spread-spectrum* (TH-SS) to simultaneously suppress interference and enable both two-way wireless IT and one-way wireless *energy transfer* (ET) in coexisting backscatter reader-tag links. The performance analysis of the BackCom network is presented, including the bit-error rates for forward and backward IT and the expected energy-transfer rate for forward ET, which account for non-coherent and coherent detection at tags and readers, and energy harvesting at tags, respectively. Our analysis demonstrates a tradeoff between energy harvesting and interference performance. Thus, system parameters need to be chosen carefully to satisfy given BackCom system performance requirement.**

I. Introduction

IoT: The *Internet-of-Things* (IoT) is an emerging network expected to connect tens of billions of smart devices in the near future, which has attracted widespread attention from both the industry and academia. One key challenge for IoT is the limited network lifetime due to the massive number of IoT devices being powered by batteries with finite capacities. *Backscatter communications* (BackCom) has emerged as a promising solution due to its low-power, low-complexity and the inherent feature of RF energy harvesting [1].

BackCom and Existing Work: Commonly adopted in RFID applications, a simple BackCom system comprises a tag and a reader. The passive tag has no active RF component and harvests energy from an unmodulated carrier wave transmitted by the reader, and modulates and reflects a fraction of the wave back to the reader [2]. The modulation relies on varying the reflection coefficient by switching between a pair of impedances. Recently, active research has been conducted on developing various types of more complex BackCom systems and networks such as wireless powered networks [3] and energy harvesting networks [4]. One particular focus of the research is techniques for multiple-access and collision avoidance in multi-tag BackCom systems [5–8]. To the best of our knowledge, simultaneous two-way information transmission BackCom and joint consideration of information-and-energy transfer have not yet been considered in the prior work.

Design Challenges: Many IoT applications e.g., e-Health and public safety, are mission critical and require low-latency communications [9]. Therefore, it is important to develop full-duplex *device-to-device* (D2D) communications between IoT devices to reduce latency as well as improve utilization of radio resources. One design related to full-duplex BackCom is proposed in [10], which supports transmission of data and control signals in the opposite directions at asymmetric rates. Such a design is incapable for supporting truly full-duplex BackCom for IoT that supports two-way links with symmetric bidirectional rates as well as provides robustness against severe inference due to the doubling of coexisting links.

In full-duplex D2D BackCom networks, interference is particularly severe due to two factors: one is the co-existence of many links and the other is the phenomenon of "interference regeneration" arising from reflection of all incident signals by each backscatter node. One interference-mitigation technique, namely *time-hopping spread spectrum* (TH-SS) [11], is particularly attractive for BackCom since its low rate provides a large processing gain and the detection of a TH-SS signal can be implemented using an energy detector available on a backscatter tag. The idea was first explored for UWB RFID (BackCom) systems in [12]. The drawback of such a system is the required sophisticated analog processing to detect ultra-sharp UWB pulses and it may not be suitable for low complexity IoT devices.

Paper Contributions: In this work, we further explore the idea to develop a practical TH-SS scheme for realizing full-duplex BackCom and simultaneous *energy transfer* (ET) in an interference network. The scheme is characterized by two key features. The first corresponds to the novel sequence-switch modulation scheme for enabling forward *information transfer* (IT) from a reader to a tag. Specifically, a bit stream is transmitted from a reader to a tag by switching between a pair of TH-SS sequences, each containing a single random nonzero chip, called an on-chip. The design has several advantages. First, the interference is suppressed by the TH-SS sequence.

This research was supported by the Australian Research Council's Discovery Project funding scheme (project number DP140101133) and supported in part by the Hong Kong Research Grants Council under Grants 17209917 and 17259416.

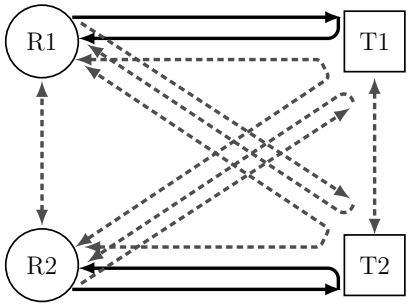

Fig. 1: Two-link full-duplex interference channel. For example, signal R2-T1-R1 is the signal transmitted by Reader 2, then backscattered by Tag 1 and received by Reader 1.

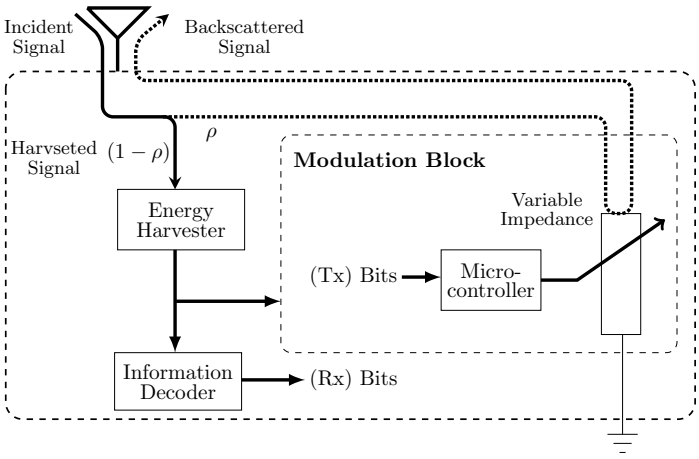

Fig. 2: The architecture of a full-duplex tag.

Second, the sequence-switch modulation is preferred to the on/off transmission in that the former ensures the existence of a non-zero chips in every symbol for the purpose of continuous forward ET. Last, the detection of data bits modulated using the proposed scheme can be realized using the on-tag energy detectors as mentioned. In addition, each tag also continuously harvests energy from interference.

As the second feature, full-duplex BackCom is realized by the modulation scheme for backward IT (tag-to-reader) where each tag modulates the on-chips in the signal from the intended reader using *binary-phase-shift keying* (BPSK), and a reader coherently detects the transmitted bits.

The performance of the proposed scheme of time-hopping full-duplex BackCom is thoroughly analyzed in this paper in terms of *bit-error rates* (BERs) for both the forward and backward IT, and the *expected energy-transfer rate* (ETR) for forward ET.

Notation: $\Pr(\mathcal{A})$ denotes the probability of the event $\mathcal{A}$. $\mathbf{1}(\mathcal{A})$ denotes the indicator function. $|\mathcal{S}|$ denotes the size (cardinality) of a set $\mathcal{S}$.

II. Network Model

Consider a BackCom interference network consisting of two coexisting single-antenna reader-tag pairs as illustrated in Fig. 1. Each reader has a conventional full-duplex antenna [13]. Each passive tag has a backscatter antenna for transmission by backscattering a fraction of the incident signal, and an energy harvester for harvesting the energy in the remaining fraction. An intended reader-tag pair communicates by full-duplex transmission with interference suppression. The design of the full-duplex tag and the interference suppression method are presented in the next section.

We assume that all the readers/tags share the same band for communication, and the channel coefficients remain unchanged within a symbol duration but may vary from symbol-to-symbol. We consider a general channel model, and also Rayleigh fading channel as a special case with both the large-scale path loss with exponent λ and the small scale Rayleigh fading. The distance between Reader m and Tag n is denoted by d_{mn}, $m, n \in \{1, 2\}$. For the reader, only the *channel state information* (CSI) of the intended backscatter channel (reader-to-tag-to-reader) is available, and the CSI of interference channels is not. The tags have no CSI of any channel. The baseband *additive white Gaussian noise* (AWGN) at Reader k, $k \in \{1, 2\}$, is represented by the random variable $z_{\text{reader},k}$ with variance σ^2_{reader}, and the passband noise signal at Tag k is $z_{\text{tag},k}(t)$ with variance σ^2_{tag}.

III. Time-Hopping Full-Duplex BackCom Scheme

In this section, we present the proposed time-hopping based multiple-access scheme and its corresponding tag architecture.

A. Architecture of Full-Duplex Tag

To enable a passive tag with simultaneous information transmission and reception, we consider the following design. The full-duplex tag consists of a power splitter, a backscatter modulation block, an energy harvester and a information detector as illustrated in Fig. 2. The incident signal is first split into two streams with a splitting ratio of ρ. The signal with ρ portion of the incident signal power is sent to the backscatter modulation block for backward IT. By switching between two mismatched impedances [2], the backscatter modulation block reflects the signal with either zero or 180-degree phase shift. Thereby, the backscattered signal is modulated with the tag's transmit bits by BPSK. Let the BPSK symbol transmitted by Tag k be denoted as q_k with $q_k \in \{1, -1\}$.

The signal with the $(1-\rho)$ fraction of the incident signal power is sent to the energy harvester for energy harvesting and energy detection based information detection. Specifically, given the RF energy harvesting efficiency η, only η portion of the RF received power is harvested. In this way, the tag transmits and receives information, and harvests energy at the same time.

B. Sequence-Switch Modulation

The proposed *sequence-switch modulation* used by each reader is presented below, which is designed for two purposes.

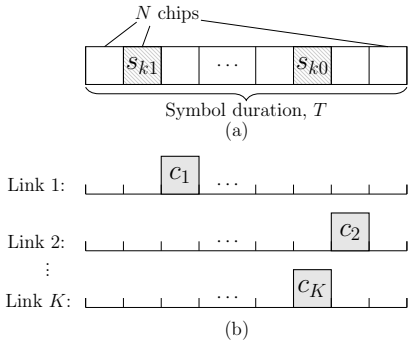

Fig. 3: Sequence-switch modulation. (a) A TH-SS pattern. (b) Transmissions of different links.

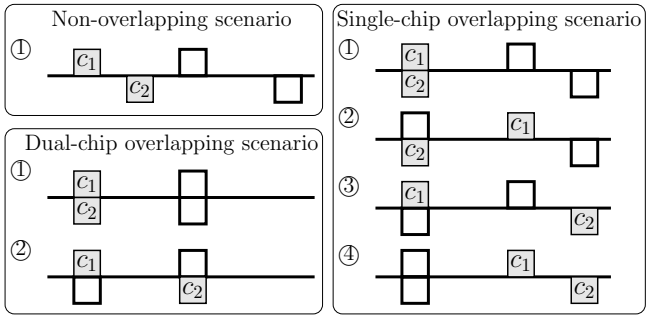

Fig. 4: Two-link pattern-overlapping scenarios and transmission cases. The pairs of on-chips of Links 1 and 2 are the squares above and under the lines, respectively.

The first is to suppress interference by TH-SS. The second is to enable simultaneous forward and backward IT and forward ET, which is further discussed in the next subsection.

Each symbol duration T is uniformly divided into N slots called *chips*. We define a *TH-SS sequence* as a N-chip random sequence comprising only a *single* randomly located nonzero chip while others are silent (i.e., zero chips). Each link, e.g., Link k, randomly chooses a pair of sequences with different nonzero *on-chips*, s_{k0} and s_{k1}, to represent bit "0" and "1", respectively. Thus, the bit stream of the reader is modulated by switching the sequences.

Specifically, the set $\mathcal{S}_k \triangleq \{s_{k0}, s_{k1}\}$ consisting of a pair of on-chips is named as a *TH-SS pattern* [see Fig. 3(a)], while all the other chips are the *off-chips*. Note that there are $\frac{N(N-1)}{2}$ available patterns in total. The transmission of a single bit by Reader k is equivalently represented by a random variable C_k with binary support $\mathcal{S}_k$, called a *transmitted on-chip*. Thus, the transmission of Reader k in an arbitrary symbol duration can be represented by a set of i.i.d. random variables $\{C_k\}$ and illustrated in Fig. 3(b).

It is clear that the interference from coexisting link occurs only when the TH-SS patterns of the two links overlap, i.e., $|\mathcal{S}_1 \cap \mathcal{S}_2| > 0$. By increasing the *sequence length* N (the processing gain), the patterns become increasingly sparse and different links are more likely to choose different patterns, i.e., the likelihood of pattern overlapping reduces, and the interference is suppressed. The *non-overlapping* ($|\mathcal{S}_1 \cap \mathcal{S}_2| = 0$), *single-chip overlapping* ($|\mathcal{S}_1 \cap \mathcal{S}_2| = 1$), and *dual-chip overlapping* ($|\mathcal{S}_1 \cap \mathcal{S}_2| = 2$) scenarios are illustrated in Fig. 4.

C. Full-Duplex BackCom

Based on the sequence-switch modulation scheme, the full-duplex BackCom is realized by the joint operation of the intended reader and tag designed as follows.

Reader-side operations: The reader transmits a forward bit to the tag using the sequence-switch modulation by sending a carrier wave represented by $\sqrt{2\mathcal{P}}\Re\{e^{j\omega t}\}$ during the on-chip, where $\mathcal{P}$ is the transmission power and ω is the angular frequency. At the same time, assuming chip-level synchronization between the reader and the tag, the reader receives the tag's backscattered BPSK signal. After cancelling the self-interference from its transmission[2], the reader detects the backward bit stream by BPSK demodulation in the intervals corresponding to the transmitted on-chip that are known to the reader.

Tag-side operations: In the two on-chips of the assigned TH-SS pattern, the tag connects the modulation block (see Fig. 2) and performs backscatter modulation, energy harvesting and information detection. Specifically, the tag detects a forward bit by *comparing* the amounts of energy harvested in the two on-chips using the energy detector. If the harvested energy in the chip s_{k0} is larger than that in the chip s_{k1}, the estimated bit is "0"; otherwise, it is "1". Note that interference signal in either one or two of the on-chips may result in detection error of the forward bit. In the off-chips of the TH-SS pattern, the tag disconnects the modulation block and harvests energy from the other reader's transmission.

Therefore, such reader and tag operations realize the full-duplex BackCom with symmetric backward and forward IT rates, and also forward ET and energy harvesting.

IV. Error Rates and Energy Transfer Efficiency

We analyze the BERs for the backward and forward IT, and the expected ETR for the forward ET of the two-link BackCom system as shown in Fig. 1. The analysis focuses on the typical link, Link 1, without loss of generality. For simplicity, we assume that all the readers and the tags are perfectly synchronized at the chip level. For the case of asynchronous transmissions, please see [14].

A. BER at the Reader for Backward IT

Consider demodulation and detection of an arbitrary bit at Reader 1, and the interference regeneration phenomenon that a backscattering tag induces interference to the other reader-

[2]It is assumed that self-interference (from transmission to reception) at the reader due to the use of a full-duplex antenna is perfectly cancelled, since the reader only transmits an unmodulated signal (i.e., the carrier wave), and the self-interference which can be easily cancelled by filtering in the analog domain [14].

tag pair. The received baseband signal at Reader 1 during its transmitted on-chip C_1 can be written as

$$r_1 = \sqrt{\mathcal{P}} f_{11} \sqrt{\rho} b_{11} q_1 + \mathbf{1}\left(C_1 \in \mathcal{S}_2\right) \sqrt{\mathcal{P}} f_{12} \sqrt{\rho} b_{21} q_2 + \mathbf{1}\left(C_1 = C_2\right) \sqrt{\mathcal{P}} (h_{21} + f_{21} \sqrt{\rho} b_{11} q_1 + f_{22} \sqrt{\rho} b_{21} q_2) + z_{\text{reader},1}, \tag{1}$$

where the two indicator functions indicate whether Tag 2 is backscattering and whether Reader 2 is transmitting during Reader 1's transmitted on-chip C_1, respectively. b_{mn} is the backward channel coefficient between Tag m and Reader n. f_{mn} is the forward channel coefficient between Reader m and Tag n. h_{mn} is the channel coefficient between Readers m and n, while g_{mn} is the channel coefficient between Tags m and n. We also assume $f_{mn} = b_{nm}^*$, i.e., the channel reciprocity. The first term and the second term in (1) correspond to the intended signal R1-T1-R1 and the interference signal R1-T2-R1, respectively, and the third term the interference signals R2-R1, R2-T1-R1, and R2-T2-R1 (see Fig. 1).

Given interference at Reader 1, the BER of coherent detection can be close to the maximum of 0.5, and is thus assumed as 0.5 as long as Reader 1 suffers interference for simplicity. Then the BER at Reader 1 is given by

$$\begin{aligned} P_{\text{reader}} &= P_{\text{BPSK}} \Pr\left(C_1 \notin \mathcal{S}_2\right) + 0.5 \Pr\left(C_1 \in \mathcal{S}_2\right) \\ &= P_{\text{BPSK}} \left(p_0 + \frac{p_1}{2}\right) + \frac{1}{2}\left(\frac{p_1}{2} + p_2\right), \end{aligned} \tag{2}$$

where P_{BPSK} denotes the BER for BPSK detection without interference, and together with the probabilities $\{p_0, p_1, p_2\}$ are defined and calculated as follows:

$$\begin{aligned} P_{\text{BPSK}} &= \mathbb{E}\left[Q\left(\sqrt{2\mathcal{P}\rho |f_{11} b_{11}|^2 / \sigma^2_{\text{reader}}}\right)\right], \\ p_0 &\triangleq \Pr\left(|\mathcal{S}_1 \cap \mathcal{S}_2| = 0\right) = \frac{(N-2)(N-3)}{N(N-1)}, \\ p_1 &\triangleq \Pr\left(|\mathcal{S}_1 \cap \mathcal{S}_2| = 1\right) = \frac{4(N-2)}{N(N-1)}, \\ p_2 &\triangleq \Pr\left(|\mathcal{S}_1 \cap \mathcal{S}_2| = 2\right) = \frac{2}{N(N-1)}. \end{aligned} \tag{3}$$

Substituting (3) into (2), the BER for the backward IT at the reader is obtained:

Proposition 1. The expected BER for the backward IT is

$$P_{\text{reader}} = \frac{N-2}{N} P_{\text{BPSK}} + \frac{1}{N}, \tag{4}$$

where for Rayleigh fading channel, it can be derived straightforwardly based on the channel-coefficient statistics that

$$P_{\text{BPSK}} = \frac{1}{2}\left(1 - \exp\left(\frac{d_{11}^{2\lambda} \sigma^2_{\text{reader}}}{4\mathcal{P}\rho}\right) \text{erfc}\left(\frac{d_{11}^{\lambda}}{2}\sqrt{\frac{\sigma^2_{\text{reader}}}{\mathcal{P}\rho}}\right)\right), \tag{5}$$

and $Q(\cdot)$ and $\text{erfc}(\cdot)$ are the Q-function and the complementary error function, respectively.

Remark 1. *The BER for the backward IT decreases with the increasing reflection coefficient ρ. For the high SNR regime ($\mathcal{P}/\sigma^2_{reader} \to \infty$), the BER reduces to $P_{reader} \approx \frac{1}{N}$, which is caused by the interference and decreases inversely with the TH-SS sequence length N. For the large sequence length scenario ($N \to \infty$), the asymptotic BER is $P_{reader} \approx \frac{N-2}{N} P_{BPSK}$, and noise is the dominant factor for causing detection errors.*

B. BER at the Tag for Forward IT

We investigate the BER at Tag 1 in three different TH-SS pattern overlapping scenarios, i.e., $|\mathcal{S}_1 \cap \mathcal{S}_2| = 0$, $|\mathcal{S}_1 \cap \mathcal{S}_2| = 1$ and $|\mathcal{S}_1 \cap \mathcal{S}_2| = 2$. Assuming that $P_{\text{tag}}^{(0)}$, $P_{\text{tag}}^{(1)}$ and $P_{\text{tag}}^{(2)}$ are the BER conditioned on the three scenarios, respectively, the BER at Tag 1 is

$$P_{\text{tag}} = \sum_{n=0}^{2} p_n P_{\text{tag}}^{(n)}. \tag{6}$$

We further calculate $P_{\text{tag}}^{(n)}$ as follows (see pattern-overlapping scenarios in Fig. 4):

1) BER Given Non-Overlapping Scenario: Tag 1's received passband signal and the received signal power in the transmitted on-chip C_1 are given by, respectively,

$$y_1(t) = \sqrt{2\mathcal{P}\eta(1-\rho)} \Re\{f_{11} e^{j\omega t}\} + z_{\text{tag},1}(t), \tag{7}$$

$$\mathcal{P}_{\text{rx}}^{(0)} = \mathcal{P}\eta(1-\rho)|f_{11}|^2 \triangleq \mathcal{P}_0. \tag{8}$$

Since neither Reader 1 nor Reader 2 is transmitting during the other on-chip $\mathcal{S}_1 \backslash C_1$, the received signal power in the other on-chip is $\breve{\mathcal{P}}_{\text{rx}}^{(0)} = 0$.

Scaling by the two-side power spectrum density of noise signal $z_{\text{tag},1}(t)$ [15], the received energy during the transmitted on-chip C_1, E_1, follows a non-central chi-square distribution with two degrees of freedom and parameter $\gamma = \mathcal{P}_0/\sigma^2_{\text{tag}}$, i.e., $\chi'^2(\gamma)$. Similarly, the scaled received energy during the other on-chip $\mathcal{S}_1 \backslash C_1$, $\breve{E}_1$, follows $\chi'^2(0)$. Therefore, comparing the scaled received energy between the on-chips C_1 and $\mathcal{S}_1 \backslash C_1$, i.e., E_1 and $\breve{E}_1$, the detection error probability is

$$P_{\text{tag}}^{(0)} = \Pr\left(\breve{E}_1 > E_1\right) = 1 - \int_0^{\infty} F_{\breve{E}_1}(x) f_{E_1}(x) \mathrm{d}x, \tag{9}$$

where $F_{\breve{E}_1}(\cdot)$ and $f_{E_1}(\cdot)$ are the cumulative distribution function (cdf) and the probability density function (pdf) of the distributions $\chi'^2(0)$ and $\chi'^2(\mathcal{P}_0/\sigma^2_{\text{tag}})$, respectively.

For tractability, we consider the high SNR regime which means $\mathcal{P}/\sigma^2_{\text{tag}} >> 0$, and ignore the noise effect on information detection, i.e., the detection is simply based on the comparison of the received signal power. Therefore, the BER in (9) is represented as

$$P_{\text{tag}}^{(0)} = \Pr\left(\breve{\mathcal{P}}_{\text{rx}}^{(0)} > \mathcal{P}_{\text{rx}}^{(0)}\right) = \Pr\left(0 > \mathcal{P}_0\right) = 0. \tag{10}$$

2) BER Given Single-Chip Overlapping Scenario: There are four transmission cases each with the same probability as illustrated in Fig. 4:

Case 1: Readers 1 and 2 are using the overlapping chip for transmission. Thus, Tag 1's received signal in the transmitted on-chip C_1 consists of four signals, i.e., R1-T1, R1-T2-T1,

$$P_{\text{tag}} = \frac{1}{N} - \frac{N-2}{N(N-1)} \frac{1}{\rho} \left(\frac{d_{22} d_t}{d_{11}}\right)^{\lambda} \exp\left(\frac{d_t^{\lambda}}{\rho}\left(\left(\frac{d_{22}}{d_{21}}\right)^{\lambda} + \left(\frac{d_{22}}{d_{11}}\right)^{\lambda}\right)\right) \Gamma\left(0,\ \frac{d_t^{\lambda}}{\rho}\left(\frac{d_{22}}{d_{21}}\right)^{\lambda} + \left(\frac{d_{22}}{d_{11}}\right)^{\lambda}\right)$$
$$- \frac{1}{N(N-1)} \left(\frac{d_{22}^{\lambda}}{d_{12}^{\lambda} + d_{22}^{\lambda}} + \frac{d_t^{\lambda}}{\rho} \frac{\frac{1}{d_{11}^{\lambda} d_{22}^{\lambda}} - \frac{1}{d_{21}^{\lambda} d_{12}^{\lambda}}}{\left(\frac{1}{d_{12}^{\lambda}} + \frac{1}{d_{22}^{\lambda}}\right)^2} \exp\left(\frac{d_t^{\lambda}}{\rho} \frac{\frac{1}{d_{11}^{\lambda}} + \frac{1}{d_{21}^{\lambda}}}{\frac{1}{d_{12}^{\lambda}} + \frac{1}{d_{22}^{\lambda}}}\right) \Gamma\left(0,\ \frac{d_t^{\lambda}}{\rho} \frac{\frac{1}{d_{11}^{\lambda}} + \frac{1}{d_{21}^{\lambda}}}{\frac{1}{d_{12}^{\lambda}} + \frac{1}{d_{22}^{\lambda}}}\right) \right), \tag{22}$$

where d_t is the distance between Tags 1 and 2, and $\Gamma(\cdot,\cdot)$ is the incomplete gamma function.

R2-T1 and R2-T2-T1, and the received signal power in the chip C_1 is

$$\mathcal{P}_{\text{rx}}^{(1)}(C_1 = C_2 = \mathcal{S}_1 \cap \mathcal{S}_2) = \eta(1-\rho)\mathcal{P}\left|f_{11} + f_{12}\sqrt{\rho} g_{21} q_2 + f_{21} + f_{22}\sqrt{\rho} g_{21} q_2\right|^2 \triangleq \mathcal{P}_1, \tag{11}$$

while the received signal power in the chip $\mathcal{S}_1 \backslash C_1$ is $\breve{\mathcal{P}}_{\text{rx}}^{(1)}(C_1 = C_2 = \mathcal{S}_1 \cap \mathcal{S}_2) = 0$. Similar with (10), the BER is

$$P_{\text{tag}}^{(1)}(C_1 = C_2 = \mathcal{S}_1 \cap \mathcal{S}_2) = \Pr(0 > \mathcal{P}_1) = 0. \tag{12}$$

Case 2: Readers 1 and 2 are using the non-overlapping chip and the overlapping chip for transmission, respectively. The received signal in the chip C_1 is signal R1-T1, since both Reader 2 and Tag 2 are not transmitting in the chip. Thus, the received signal power in the chip C_1 is the same with (8), i.e., $\mathcal{P}_{\text{rx}}^{(1)}(C_1 \neq C_2 = \mathcal{S}_1 \cap \mathcal{S}_2) = \mathcal{P}_0$. While the received signal in $\mathcal{S}_1 \backslash C_1$ consists of signals R2-T1 and R2-T2-T1, and

$$\breve{\mathcal{P}}_{\text{rx}}^{(1)}(C_1 \neq C_2 = \mathcal{S}_1 \cap \mathcal{S}_2) = \eta(1-\rho)\mathcal{P}\left|f_{21} + f_{22}\sqrt{\rho} g_{21} q_2\right|^2 \triangleq \mathcal{P}_2. \tag{13}$$

Thus, the BER is

$$P_{\text{tag}}^{(1)}(C_1 \neq C_2 = \mathcal{S}_1 \cap \mathcal{S}_2) = \Pr(\mathcal{P}_2 > \mathcal{P}_0). \tag{14}$$

Case 3: Readers 1 and 2 are using the overlapping chip and the non-overlapping chip for transmission, respectively. The received signal in the chip C_1 consists of two signals, R1-T1 and R1-T2-T1, thus, the received signal power in the chip is

$$\mathcal{P}_{\text{rx}}^{(1)}(C_2 \neq C_1 = \mathcal{S}_1 \cap \mathcal{S}_2) = \eta(1-\rho)\mathcal{P}\left|f_{11} + f_{12}\sqrt{\rho} g_{21} q_2\right|^2 \triangleq \mathcal{P}_3, \tag{15}$$

and the received signal power in the chip $\mathcal{S}_1 \backslash C_1$ is $\breve{\mathcal{P}}_{\text{rx}}^{(1)}(C_2 \neq C_1 = \mathcal{S}_1 \cap \mathcal{S}_2) = 0$. Thus, the BER is

$$P_{\text{tag}}^{(1)}(C_2 \neq C_1 = \mathcal{S}_1 \cap \mathcal{S}_2) = \Pr(0 > \mathcal{P}_3) = 0. \tag{16}$$

Case 4: Readers 1 and 2 are using non-overlapping chips for transmission. The received signal power in the chips C_1 and $\mathcal{S}_1 \backslash C_1$ are $\mathcal{P}_0$ and 0, respectively, and thus,

$$P_{\text{tag}}^{(1)}(C_1 \neq \mathcal{S}_1 \cap \mathcal{S}_2, C_2 \neq \mathcal{S}_1 \cap \mathcal{S}_2) = \Pr(0 > \mathcal{P}_0) = 0. \tag{17}$$

3) BER Given Dual-Chip Overlapping Scenario: There are two transmission cases each with the same probability as illustrated in Fig. 4:

Case 1: Readers 1 and 2 are using the same chip for transmission. We see that the received signal power in the chips C_1 and $\mathcal{S}_1 \backslash C_1$ are $\mathcal{P}_1$ and 0, respectively, and thus,

$$P_{\text{tag}}^{(2)}(C_1 = C_2) = \Pr(0 > \mathcal{P}_1) = 0. \tag{18}$$

Case 2: Readers 1 and 2 are using different chips for transmission. The received signal in the chip C_1 consists of signals R1-T1 and R1-T2-T1, thus, the received signal power in the non-overlapping chip is the same with (15), i.e., $\mathcal{P}_{\text{rx}}^{(2)}(C_1 \neq C_2) = \mathcal{P}_3$. While the received signal in $\mathcal{S}_1 \backslash C_1$ consists of signals R2-T1 and R2-T2-T1 which is the same with (13), i.e., $\breve{\mathcal{P}}_{\text{rx}}^{(2)}(C_1 \neq C_2) = \mathcal{P}_2$. Thus, the BER is

$$P_{\text{tag}}^{(2)}(C_1 \neq C_2) = \Pr(\mathcal{P}_2 > \mathcal{P}_3). \tag{19}$$

4) Main Results and Discussions: Based on (6), the expected BER for the forward IT is

$$P_{\text{tag}} = \frac{N-2}{N(N-1)} \Pr(\mathcal{P}_2 > \mathcal{P}_0) + \frac{1}{N(N-1)} \Pr(\mathcal{P}_2 > \mathcal{P}_3)$$
$$= \frac{N-2}{N(N-1)} \Pr\left(\left|f_{21} + f_{22}\sqrt{\rho} g_{21} q_2\right|^2 > \left|f_{11}\right|^2\right)$$
$$+ \frac{1}{N(N-1)} \Pr\left(\left|f_{21} + f_{22}\sqrt{\rho} g_{21} q_2\right|^2 > \left|f_{11} + f_{12}\sqrt{\rho} g_{21} q_2\right|^2\right). \tag{20}$$

Thus, as the sequence length $N \to \infty$,

$$P_{\text{tag}} \approx \frac{1}{N} \Pr\left(\left|f_{21} + f_{22}\sqrt{\rho} g_{21} q_2\right|^2 > \left|f_{11}\right|^2\right). \tag{21}$$

Remark 2. *From* (21)*, we see that the BER for the forward IT can be reduced by increasing the sequence length* N.

For Rayleigh fading channel, considering the randomness of the channel coefficients and q_2, it is straightforward to obtain the following result.

Proposition 2. For Rayleigh fading channel, the expected BER for the forward IT is given in (22), shown at the top of this page.

Remark 3. *For the typical case that each reader-tag pair distance is smaller than the cross reader-tag distance, i.e.,* $d_{11} < d_{21}$ *and* $d_{22} < d_{12}$*, we have* $\frac{1}{d_{11}^{\lambda} d_{22}^{\lambda}} - \frac{1}{d_{21}^{\lambda} d_{12}^{\lambda}} > 0$ *in* (22)*, and thus, it can be shown that* P_{tag} *monotonically increases with* ρ*. Therefore, a higher reflection coefficient leads to a higher BER for the forward IT, and there is a tradeoff between the BERs for the forward and backward transmission in terms of* ρ*.*

C. Expected ETR at the Tag for Forward ET

We analyze the expected ETR taken into account the harvested energy at Tag 1 during the on-chips and the off-chips. For the pair of on-chips, we have analyzed the harvested power

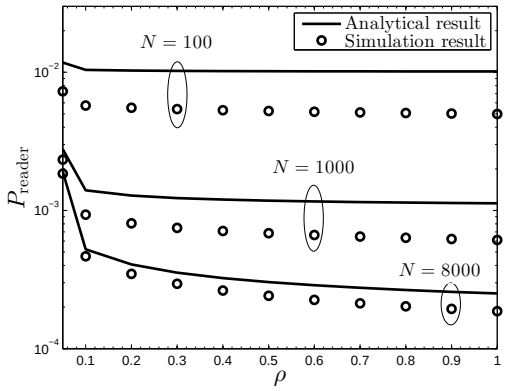

Fig. 5 Reader BER for different reflection coefficients.

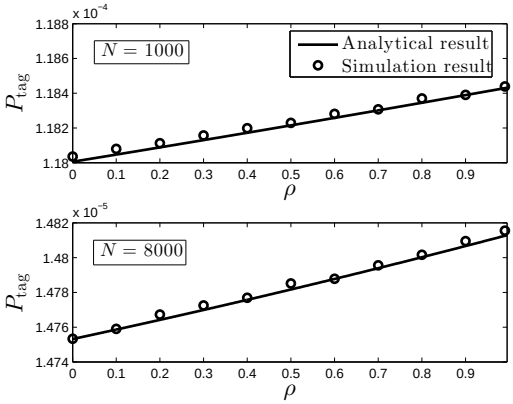

Fig. 6 Tag BER for different reflection coefficients.

(energy) in Section IV-B. While for the off-chips, Tag 1 can harvest energy from Reader 2's IT and Tag 2's backscattering only if $C_2 \notin \mathcal{S}_1$ with the probability $\Pr(C_2 \notin \mathcal{S}_1) = p_0 + \frac{1}{2}p_1$. Given $C_2 \notin \mathcal{S}_1$, Tag 1's received signal in the chip C_2 consists of two signals, i.e., R2-T1 and R2-T2-T1, and the received signal power in the chip is

$$\mathcal{P}_{\text{eh}} \triangleq \eta \mathcal{P} \left| f_{21} + f_{22}\sqrt{\rho} g_{21} q_2 \right|^2. \tag{23}$$

Therefore, considering Tag 1's received signal power in the chips C_1, $\mathcal{S}_1 \backslash C_1$ and C_2 based on the analysis in Section IV-B and (23), the expected ETR is[3]

$$\begin{aligned}\mathcal{E}_{\text{tag}} &= \frac{T}{N}\left(\sum_{n=0}^{2} p_n \mathbb{E}\left[\mathcal{P}_{\text{rx}}^{(n)} + \breve{\mathcal{P}}_{\text{rx}}^{(n)}\right] + \Pr(C_2 \notin \mathcal{S}_1)\,\mathbb{E}\left[\mathcal{P}_{\text{eh}}\right]\right) \\ &= \frac{T}{N}\mathbb{E}_{f_{11},f_{12},f_{21},f_{22},g_{21},q_2}\left[\frac{N-2}{N}\left(\mathcal{P}_0 + \mathcal{P}_{\text{eh}}\right) \right. \\ &\qquad \left. + \frac{1}{N}\left(\mathcal{P}_1 + \mathcal{P}_2 + \mathcal{P}_3\right)\right].\end{aligned} \tag{24}$$

Remark 4. *It is observed that the expected ETR decreases with the sequence length N and approaches zero, since the readers only have very short on-chip duration for active transmission.*

Proposition 3. For Rayleigh fading channel, the expected ETR is

$$\mathcal{E}_{\text{tag}} = \frac{\eta \mathcal{P} T}{N}\left(\nu_1 \rho^2 + \nu_2 \rho + \nu_3\right), \tag{25}$$

where

$$\begin{aligned}&\nu_1 = -\frac{2}{N}\left(\frac{1}{d_{12}^{\lambda} d_t^{\lambda}} + \frac{1}{d_{22}^{\lambda} d_t^{\lambda}}\right),\ \nu_3 = \frac{1}{d_{11}^{\lambda}} + \frac{1}{d_{21}^{\lambda}}, \\ &\nu_2 = \frac{2}{N}\left(\frac{1}{d_{12}^{\lambda} d_t^{\lambda}} - \frac{1}{d_{21}^{\lambda}}\right) + \frac{1}{d_{22}^{\lambda} d_t^{\lambda}} - \frac{1}{d_{11}^{\lambda}}.\end{aligned} \tag{26}$$

The proof is straightforward and omitted for brevity.

[3]Note that we have included all channel coefficients as the potential random variables over which the expectation is taken.

Remark 5. *Thus, for the typical case that $d_{12}d_t >> d_{21}$ and $d_{22}d_t >> d_{11}$, the expected ETR $\mathcal{E}_{tag}$ increases inversely with ρ for Rayleigh fading channel.*

V. Numerical Results

In this section, we numerically present the performance of the proposed full-duplex time-hopping BackCom in the Rayleigh fading channel scenario. We set the path loss exponent as $\lambda = 2.5$, and the distance (in meters) between the devices as $d_{11} = 10$, $d_{22} = 10$, $d_t = 20$, $d_{12} = 22$, and $d_{21} = 22$. Also we set the reader transmit power as $\mathcal{P} = 50$ mW, the noise variance at the reader and the tag as $\sigma^2_{\text{reader}} = \sigma^2_{\text{tag}} = -100$ dBm, and the RF energy harvesting efficiency as $\eta = 0.5$.

In the following, we plot the BERs for the forward and backward IT (i.e., P_{reader} and P_{tag}), and the expected ETR (i.e., $\mathcal{E}_{\text{tag}}$) for the forward ET based on the analytical results derived in Section IV. The Monte Carlo simulation results, averaged over 10^9 random channel realizations, are also presented. Specifically, the modeling assumptions for the analytical results of BER for the forward and backward IT in Section IV are verified by the simulation results.

Model Validation: In Fig. 5, P_{reader} is plotted using Proposition 1 for different sequence length N and reflection coefficient ρ. We see that the analytical result is an upper bound of the simulation result, and the gap diminishes as N increases, e.g., qualitatively that the analysis becomes reasonably accurate when $N = 8000$. Thus, the analytical result based on the assumption that the BER at the reader is 0.5 as long as the reader suffers from interference, is a tight upper bound especially when N is large.

In Fig. 6, P_{tag} is plotted using Proposition 2 for different N and ρ. We see that the analytical result perfectly matches the simulation result, which verifies that the modeling assumption of negligible noise effect on the forward BER is accurate under the practical settings.

In Fig. 7, the curves of the normalized expected ETR for the forward ET, $\mathcal{E}_{\text{tag}}/T$, are plotted using Proposition 3 for different ρ and N. The analytical result perfectly matches the simulation result.

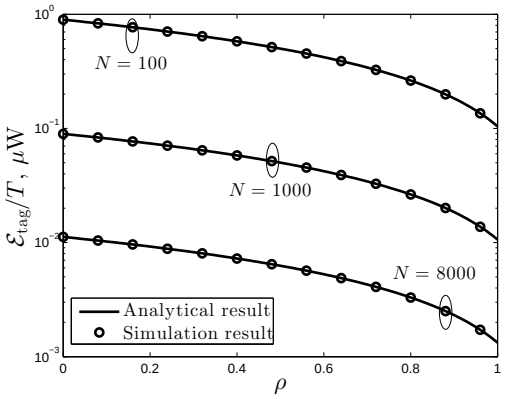

Fig. 7 Expected ETR for different reflection coefficients.

Design Insights: From Figs. 5-7, it is observed that P_{reader} decreases while P_{tag} and $\mathcal{E}_{\text{tag}}$ increase with increasing ρ. This is because a larger ρ induces a stronger backscattered signal and a weaker received signal at the tag, which enhances the SNR of the backward IT but reduces the performance of the forward IT and ET. We see that P_{reader}, P_{tag} and $\mathcal{E}_{\text{tag}}$ decreases with increasing N. This is because a larger sequence length N reduces the pattern-overlapping probability and hence suppresses the interference for both the forward and backward IT. However, it makes the readers have a shorter time (i.e., a shorter on-chip duration) for active transmissions, and hence reduces the performance of the forward ET.

Therefore, for practical BackCom system design, such performance tradeoff with the design parameters, i.e., the reflection coefficient and the sequence length, should be carefully considered to satisfy the performance requirement of a certain BackCom system.

VI. Conclusions

In this paper, we have proposed a full-duplex BackCom network, where a novel TH-SS based multiple-access scheme is designed. The scheme enables simultaneous interference suppression from coexisting links and full-duplex forward/backward IT. Moreover, the scheme not only supports dedicated ET for every symbol but also enable opportunistic wireless energy harvesting from interference. Several interesting design insights are obtained, such as: a large TH-SS sequence length improves the performance of the backward and forward IT but degrades the performance of the forward ET. Thus, system parameters need to be chosen carefully to satisfy given BackCom system performance requirement.

References

[1] W. Liu, K. Huang, X. Zhou, and S. Durrani, "Next Generation Backscatter Communication: Theory and Applications," *ArXiv e-prints*, 2017. [Online]. Available: https://arxiv.org/abs/1701.07588

[2] C. Boyer and S. Roy, "Backscatter communication and RFID: Coding, energy, and MIMO analysis," *IEEE Trans. Commun.*, vol. 62, no. 3, pp. 770–785, Mar. 2014.

[3] K. Han and K. Huang, "Wirelessly powered backscatter communication networks: Modeling, coverage and capacity," *to appear in IEEE Trans. Wireless Commun.*, 2017.

[4] V. Liu, A. Parks, V. Talla, S. Gollakota, D. Wetherall, and J. R. Smith, "Ambient backscatter: Wireless communication out of thin air," in *Proc. ACM SIGCOMM*, 2013, pp. 39–50.

[5] A. Bletsas, S. Siachalou, and J. N. Sahalos, "Anti-collision backscatter sensor networks," *IEEE Trans. Wireless Commun.*, vol. 8, no. 10, pp. 5018–5029, Oct. 2009.

[6] J. Kimionis, A. Bletsas, and J. N. Sahalos, "Increased range bistatic scatter radio," *IEEE Trans. Commun.*, vol. 62, no. 3, pp. 1091–1104, Mar. 2014.

[7] A. Alma'aitah, H. S. Hassanein, and M. Ibnkahla, "Tag modulation silencing: Design and application in RFID anti-collision protocols," *IEEE Trans. Commun.*, vol. 62, no. 11, pp. 4068–4079, Nov. 2014.

[8] J. Wang, H. Hassanieh, D. Katabi, and P. Indyk, "Efficient and reliable low-power backscatter networks," in *Proc. ACM SIGCOMM*, 2012, pp. 61–72.

[9] A. Al-Fuqaha, M. Guizani, M. Mohammadi, M. Aledhari, and M. Ayyash, "Internet of Things: A survey on enabling technologies, protocols, and applications," *IEEE Commun. Surveys Tuts.*, vol. 17, no. 4, pp. 2347–2376, Fourth Quarter 2015.

[10] V. Liu, V. Talla, and S. Gollakota, "Enabling instantaneous feedback with full-duplex backscatter," in *Proc. ACM MobiCom*, 2014, pp. 67–78.

[11] M. Z. Win, R. A. Scholtz *et al.*, "Ultra-wide bandwidth time-hopping spread-spectrum impulse radio for wireless multiple-access communications," *IEEE Trans. Commun.*, vol. 48, no. 4, pp. 679–689, Apr. 2000.

[12] D. Dardari, R. D. Errico, C. Roblin, A. Sibille, and M. Z. Win, "Ultrawide bandwidth RFID: Next generation?" *Proc. IEEE*, vol. 98, no. 9, pp. 1570–1582, Sep. 2010.

[13] D. Bharadia, E. McMilin, and S. Katti, "Full duplex radios," in *Proc. ACM SIGCOMM*, 2013, pp. 375–386.

[14] W. Liu, K. Huang, X. Zhou, and S. Durrani, "Full-Duplex Backscatter Interference Networks Based on Time-Hopping Spread Spectrum," *IEEE Trans. Wireless Commun.*, vol. 16, no. 7, pp. 4361–4377, Jul. 2017.

[15] H. Urkowitz, "Energy detection of unknown deterministic signals," *Proc. IEEE*, vol. 55, no. 4, pp. 523–531, Apr. 1967.